



# Oxidative mobilization of cerium and uranium and enhanced release of “immobile” high field strength elements from igneous rocks in the presence of the biogenic siderophore desferrioxamine B

Dennis Kraemer<sup>a,\*</sup>, Sebastian Kopf<sup>a,b</sup>, Michael Bau<sup>a</sup>

<sup>a</sup> Department of Physics and Earth Sciences, Jacobs University Bremen, Campus Ring 1, 28759 Bremen, Germany

<sup>b</sup> Department of Geosciences, 152 Guyot Hall, Princeton University, Princeton, NJ 08544, USA

Received 7 November 2014; accepted in revised form 29 May 2015; available online 4 June 2015

## Abstract

Polyvalent trace elements such as the high field strength elements (HFSE) are commonly considered rather immobile during low-temperature water–rock interaction. Hence, they have become diagnostic tools that are widely applied in geochemical studies. We present results of batch leaching experiments focused on the mobilization of certain HFSE (Y, Zr, Hf, Th, U and rare earth elements) from mafic, intermediate and felsic igneous rocks in the presence and absence, respectively, of the siderophore desferrioxamine B (DFOB). Our data show that DFOB strongly enhances the mobility of these trace elements during low-temperature water–rock interaction.

The presence of DFOB produces two distinct features in the Rare Earths and Yttrium (REY) patterns of leaching solutions, regardless of the mineralogical and chemical composition or the texture of the rock type studied. Bulk rock-normalized REY patterns of leaching solutions with DFOB show (i) a very distinct positive Ce anomaly and (ii) depletion of La and other light REY relative to the middle REY, with a concave downward pattern between La and Sm. These features are not observed in experiments with hydrochloric acid, acetic acid or deionized water. In DFOB-bearing leaching solutions Ce and U are decoupled from and selectively enriched relative to light REY and Th, respectively, due to oxidation to Ce(IV) and U(VI). Oxidation of Ce<sup>3+</sup> and U<sup>4+</sup> is promoted by the significantly higher stability of the Ce(IV) and U(VI) DFOB complexes as compared to the Ce(III) and U(IV) DFOB complexes. This is similar to the relationship between the Ce(IV)- and Ce(III)-pentacarbonate complexes that cause positive Ce anomalies in alkaline lakes. However, while formation of Ce(IV) carbonate complexes is confined to alkaline environments, Ce(IV) DFOB complexes may produce positive Ce anomalies even in mildly acidic and near-neutral natural waters. Siderophore-promoted dissolution processes also significantly enhance mobility of other ‘immobile’ HFSE and may not only cause or modify Ce anomalies and Th–U fractionation, but also mobilization of and fractionation between Zr, Hf, Th and redox-insensitive REY during weathering, pedogenesis, diagenesis and incongruent dissolution of particles in seawater and freshwater.

Siderophores may significantly affect the use of HFSE as geochemical tools. Concave downward light REY patterns may be used as a biosignature for water–rock interaction in the presence of siderophores. Enhanced and preferential mobilization of U relative to Th in the presence of siderophores may produce Th–U signals comparable to those indicative of weathering under oxidized conditions, which might constrain the use of U concentrations and Th/U ratios as a paleoredox-proxy. The enhanced mobilization of Zr and especially Hf from igneous rocks in the presence of DFOB might have implications for the use of the latter as a tracer for the impact of continental weathering on seawater chemistry. Because siderophore complexes affect the particle-reactivity of Hf and Zr, they may prevent effective removal of terrigenous Hf and Zr during

\* Corresponding author.

E-mail address: [d.kraemer@jacobs-university.de](mailto:d.kraemer@jacobs-university.de) (D. Kraemer).

aggregation/coagulation of riverine particles in estuaries. Siderophore-promoted solubilization and stabilization might hence be an additional way to transport continental Hf and Zr to the oceans. Furthermore, siderophore-enhanced mobilization may also have implications for the remediation techniques employed to immobilize HFSE such as U, Th and REY, at nuclear waste and reprocessing sites and at REY ore processing plants, where soils are commonly contaminated with these (sometimes radioactive) heavy metals.

© 2015 Elsevier Ltd. All rights reserved.

## 1. INTRODUCTION

The distribution and behavior of large ion lithophile elements such as Rb, Sr and Cs, and of high field strength elements (HFSE) such as the rare earth elements and Y (REY), Zr, Hf, Th and U, in igneous systems are predominantly controlled by their charge and ionic size (Goldschmidt, 1937). Hence, isoivalent elements with similar ionic radii (e.g., geochemical twins like  $Y^{3+}$ – $Ho^{3+}$ ) display coherent behavior and maintain a chondritic ratio during igneous processes. The term *CHARAC* (CHarge And RADIUS Controlled; Bau, 1996) was introduced for geochemical processes which do not fractionate geochemical twins such as Y–Ho, Zr–Hf, and Nb–Ta, or element pairs like Th and U. Most igneous processes, except for those operating in highly evolved silicate melts, are considered as *CHARAC* processes. In contrast, non-*CHARAC* trace element behavior is common in aqueous systems and in igneous systems involving large amounts of volatiles such as  $H_2O$  and others (Bau, 1996). The most common reason for non-*CHARAC* behavior of trace elements in aqueous systems is chemical complexation with inorganic and/or organic ligands.

The REY have very similar physico-chemical properties and are in natural systems, with the exception of Ce and Eu, exclusively trivalent. This leads to very coherent behavior of the REY in geochemical systems and processes. Thus, the REY have become a powerful tools in both igneous and aqueous geochemistry. However, attempts to employ anomalous HFSE patterns as quantitative indicators for specific geochemical conditions are often hampered by limited knowledge of the various processes that can produce such anomalies. For example, the REY are exclusively trivalent in low-temperature systems with the notable exception of Ce which may be oxidized and form Ce(IV) compounds. Cerium oxidation may lead to the decoupling of Ce from its trivalent neighbors in the REY series, resulting in the formation of positive or negative Ce anomalies in normalized REY patterns. The absence or presence of Ce anomalies has been used as a qualitative redox proxy, but any attempt to establish Ce-REY decoupling as a quantitative proxy suffers from limited knowledge of the various parameters that affect the redox behavior of Ce in natural systems.

Organic matter and organic chelators in general have been shown to be among the key factors controlling REY and HFSE speciation and mobilization in the critical zone at or near the Earth's surface and, particularly, in aquatic environments such as groundwaters, rivers, lakes and soil solutions (e.g., Gruau et al., 2004; Davranche et al., 2004,

2008; Neaman et al., 2005; Pourret et al., 2007). In this study, we focus on the chelation effects of siderophores to elucidate the potential role that this important group of organic ligands may play for the behavior of the HFSE during low-temperature water–rock interactions.

Siderophores are a group of chemically diverse low-molecular weight organic ligands with extraordinarily high binding affinities for  $Fe^{3+}$ . They are produced by bacteria, fungi and plants to cope with the scarcity of bioavailable iron in the environment (Boukhalfa and Crumbliss, 2002), and constitute one of the most important groups of biogenic organic ligands in many terrestrial and marine environments. Most of the various siderophores known today incorporate hydroxamic acid, catechol and/or carboxyl functional groups (Albrecht-Gary and Crumbliss, 1998; Kraemer, 2004; Kalinowski et al., 2004) and are highly efficient complexing agents for polyvalent metal ions besides Fe. Many studies have highlighted this important side-effect of siderophores on metal (de)sorption and complexation processes (e.g., Yoshida et al., 2004, 2007; Ozaki et al., 2006; Bau et al., 2013), with few publications aimed specifically at HFSE, platinum group elements (PGE) and the actinides. Dahlheimer et al. (2007) published an extensive study on the siderophore-promoted mobility of platinum group elements in surface environments and found that the siderophore desferrioxamine B (DFOB) is likely to increase the mobility of Pt and Pd in soils. The study conducted by Dahlheimer et al. (2007) focused on the solubility of Pt, Pd and Rh metal and oxides in batch experiments. The potential competition of PGE with e.g., Fe(III) for DFOB complexation was not considered in these batch experiments, and therefore, the DFOB-promoted solubility of PGE is likely much lower in (natural) systems with competing cations that form more stable complexes with DFOB than the PGE. Kraemer et al. (2015) showed that DFOB is a promising reagent for the hydrometallurgical extraction of Pt and Pd from oxidized platinum group element ores. Yoshida et al. (2007) demonstrated very effective complexation with DFOB and subsequent solubilization of Hf, while Brainard et al. (1992) and Bouby et al. (1998) demonstrated this for the actinides. Christenson and Schijf (2011) published a dataset of experimentally obtained stability constants for REY(III) at seawater ionic strength (Fig. 1) and found that REY-DFOB complexes are many orders of magnitude more stable than REY complexes with carbonate which is the most important inorganic REY-complexing ligand in seawater.

Previous work on volcanic ash-rich glacial meltwaters from Iceland (Bau et al., 2013) also found that the presence of siderophores in solution significantly enhances the

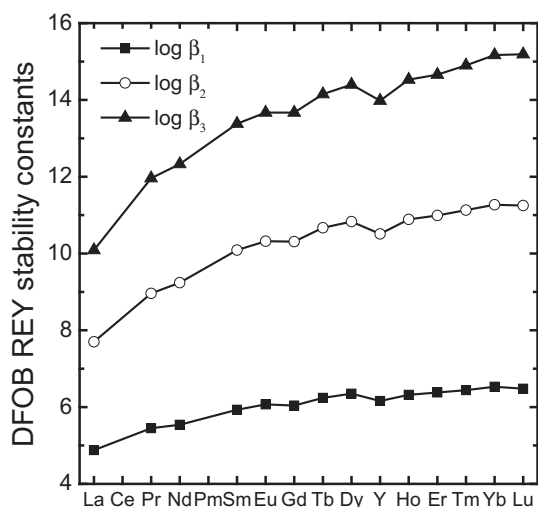


Fig. 1. Stability constants of bi- ( $\log \beta_1$ ), tetra- ( $\log \beta_2$ ) and hexadentate ( $\log \beta_3$ ) complexes of the REY with the siderophore desferrioxamine B at seawater ionic strength (data from Christenson and Schijf, 2011). Note that the difference between the stabilities of light and middle REY(III) DFOB complexes is much more pronounced than that between middle and heavy REY(III) DFOB complexes.

transfer of rare earth elements (REE) from the particulate to the dissolved fraction, suggesting that the presence of siderophores in natural systems actively modifies the concentrations and distribution of dissolved REE in the surface environment despite high abundances of (dissolved) Fe in the meltwaters and in the mafic volcanic ash, which competed with the REE for complexation with the DFOB ligand.

These observations highlighted the need for a more systematic investigation of the actual impact of siderophores on the mobilization and fractionation of HFSE and REY during weathering processes. Here, we present results from batch leaching experiments with the siderophore DFOB on a range of mafic, intermediate and felsic igneous rocks to assess the impact of siderophores specifically on the mobility of HFSE and REY during weathering. Desferrioxamine B is a common siderophore in aerobic soils (Müller et al., 1984; Rosenberg and Maurice, 2003), that forms metal complexes through coordination with hydroxamate functional groups (Dhungana et al., 2001), and that has been used extensively in prior work on siderophore sorption, weathering and mineral dissolution (e.g., Farkas et al., 1997; Kiss and Farkas, 1998; Liermann et al., 2000; Kraemer, 2004; Buss et al., 2007; Duckworth and Sposito, 2007; Mullen et al., 2007; Christenson and Schijf, 2011; Ohnuki and Yoshida, 2012; Bau et al., 2013; Akafia et al., 2014).

We chose a range of common igneous rock types with different chemical and mineralogical compositions and with different textures to investigate whether or not the geochemical twins Zr–Hf, Y–Ho and the elements Th and U are decoupled from each other, and whether or not a unique REY signature exists that characterizes REY mobilization in the presence of the DFOB siderophore. We also included basaltic glasses in the study to test whether or not

any of the specific features observed in the leaching experiments are due to the texture or mineralogical composition of the rocks studied.

## 2. MATERIALS AND METHODS

### 2.1. Samples

We conducted standardized incubation experiments on igneous rock samples from a variety of geologic settings. The complete sample set comprises four mid-ocean ridge basalts (MORB), two ocean island basalts (OIB), two andesites and a granite. The mineralogical composition of the rock samples is listed in Table 1.

Sample OL-20b was originally described by Schnurr (1995) and is a basaltic andesite of the Paleoproterozoic Ongeluk Formation of the Transvaal Supergroup, South Africa. The island-arc andesite sample A-Jp originates from a lava flow underlying the Nishiki-numa spring (Hokkaido, Japan) and is described by Bau et al. (1998). The mid-ocean ridge (micro-)crystalline basalts were collected during research cruises at the East Pacific Rise at 21°S (sample MORB-EPR), described previously by Giese and Bau (1994), as well as from an aphyritic sheet flow in the area of the Turtle Pits hydrothermal field of the Mid-Atlantic Ridge (MORB-TP). For details on the Turtle Pit sample, see Haase et al. (2007). The samples MORB-EPR<sub>glass</sub> and MORB-TP<sub>glass</sub> represent the outermost, glassy rim of the aforementioned MORBs, while the microcrystalline interior of these basalts is represented by samples MORB-EPR and MORB-TP, respectively. OIB-Me is a primitive alkali basalt from Mehetia Island (Society hotspot) and is discussed as sample Me90-05 by Binard et al. (1993). The second OIB sample, OIB-Haw, is a vesicular tholeiite from Kilauea, Hawaii and is also discussed by Giese and Bau (1994). The granite GSAF3 is from the Lebowa Granite Suite, Bushveld Complex, South Africa.

The rock chips were rinsed with deionized water, dried and powdered to <63 μm with a Fritsch Pulverisette-6 planetary mill with agate balls and a sealed agate mortar in order to minimize sample contamination. Bulk decomposition of the powdered rock samples was carried out using a DAS acid digestion system (Pico Trace, Germany) following the mixed acid digestion protocol outlined by Dulski (2001) and Alexander (2008).

### 2.2. Experimental

We used the siderophore desferrioxamine B (DFOB) for our experiments. DFOB is the best studied siderophore to date and easily available in its mesylate form as the drug *Desferal*<sup>®</sup> (Novartis AG) which is used to treat acute and chronic iron overload (Nick et al., 2003; Bernhardt, 2007).

Christenson and Schijf (2011) reported that, compared to DFOB complexes, REY complexes with mesylate are weak and do not influence REY behavior. Due to the relatively similar chemical properties of REY and other HFSE, mesylate interactions with investigated elements are considered negligible in comparison to HFSE- and REY-DFOB interactions.

Table 1

Mineralogical data of rock samples used for leaching experiments. Abbreviations: *Ol* = olivine, *Px* = Pyroxene, *Cpx* = clinopyroxene, *Mt* = titanomagnetite, *Plg* = plagioclase.

Sample	Mineralogy	References
OIB-Me	<i>Ol</i> and <i>Cpx</i> phenocrysts in a glassy matrix of <i>Plg</i> and <i>Mt</i> , no visible secondary minerals	Giese and Bau (1994)
OIB-Haw	Phenocrysts of <i>Ol</i> in a matrix of <i>Plg</i> , <i>Cpx</i> and glass, no visible secondary minerals	Giese and Bau (1994)
MORB-EPR	<i>Ol</i> , <i>Plg</i> and <i>Px</i> microcrystallites in a partially devitrified glassy matrix, no visible secondary minerals	Giese and Bau (1994)
MORB-TP	Microcrystalline <i>Ol</i> , <i>Plg</i> and <i>Px</i> , no visible secondary minerals	This study
A-Jp	Microcrystalline <i>Plg</i> , <i>Cpx</i> and minor <i>Ol</i> , no visible secondary minerals	Bau et al. (1998)
OL20B	Phenocrysts of <i>Plg</i> and <i>Cpx</i> in a <i>Px</i> -dominating matrix, minor amounts of sericite, chlorite and clay minerals indicate small-scale rock alteration	Schnurr (1995)
GSAF3	<i>Plg</i> , <i>Qtz</i> , minor mica, no secondary minerals	This study

The batch leaching experiments were conducted in a trace-metal clean environment with acid-cleaned labware. Aliquots of exactly 1 g of the dried and powdered igneous rock samples were weighed out into acid-cleaned LDPE bottles. The siderophore solutions were prepared separately with *Desferal*<sup>®</sup> and deionized water (DIW). The purity of *Desferal*<sup>®</sup> was checked by reagent blank measurements; trace-element concentrations in *Desferal*<sup>®</sup> were found to be at least two orders of magnitude lower than the concentrations in our experiments. Immediately after preparation of the solution, the pH of the leaching reagent was determined and the exact amount of siderophore solution matching a 20 g/l solid content and a DFOB concentration matching 1 mM was added to the bottles containing the pre-weighed sample powder. The bottles were handshaken for a minute to facilitate dispersion and then placed on a shaker table set at 180 rpm. After 24 h, the samples were taken off the shaker table and the solution was filtered using an acid-cleaned filter tower with a 0.2 µm membrane filter. The leachates were measured for pH and were then acidified with supra-pure hydrochloric acid to pH < 2 and stored for later analysis by quadrupole ICP-MS.

A time-series experiment on sample OL-20B was conducted using 500 ml LDPE bottles, 4 g of sample powder and 200 ml DFOB leaching solution. The sample was mixed with the leaching solution, handshaken for a minute to facilitate full dispersion and placed on a shaker table. The time intervals for sampling were 1, 8, 24, and 48 h. REY and HFSE concentrations increased sharply for the first 24 h and then remained approximately the same. Hence, all other experiments were done with contact times of 24 h to minimize the potential impact of readsorption phenomena. The pH was measured at each time point. Sampling was conducted on the dispersed, well-shaken sample with a syringe filter with a 0.2 µm membrane size. Sampling volume was 5 ml. After sampling, the bottle was closed and returned to the shaker table.

The leaching experiments were performed with an experiment time of 24 h in unbuffered leaching solutions to more closely resemble natural water–rock interaction. The pH values of the solutions of the batch leaching experiments increase from a starting pH of 5.5 to up to 9 (Table 3). The batch leaching experiments with OIB-Haw, MORB-TP and MORB-EPR were carried out in duplicate for quality control. The replicates demonstrate a good overall reproducibility of the experimental approach and the analysis (e.g.,

Fig. 5). To verify that the observed element mobilization patterns are characteristic for siderophore leaching, we also conducted control experiments with 1 mM HCl, 1 mM acetic acid, and DIW using the same experimental setup as for the siderophore leaching experiments.

The experimental siderophore concentrations (1 mM) used in this study are representative of very organic-rich soil systems (Kraemer, 2004) but exceed concentrations commonly encountered in natural waters and other environmental systems (typically below 10 µM). However, it should be noted that rocks in natural systems are subject to constant removal and re-supply of aqueous solutions containing a wide range of siderophores and other organic molecules. Considering the long time scales at work in natural weathering processes, the use of high siderophore concentrations is a reasonable surrogate for short-term lab-scale experiments.

### 2.3. Analytical

For whole rock analysis, exactly 50 mg of the dried sample aliquots of the rock powders (and also of certified reference materials for quality control) were pressure-digested with a concentrated acid-mixture of hydrofluoric acid, hydrochloric acid and nitric acid with a PicoTrace DAS digestion unit. All acids used for digestion and analysis were of supra-pure grade. The leachates as well as the digested bulk rock samples were measured with a Perkin-Elmer quadrupole ICP-MS ELAN drc-e. Background intensities of procedural blanks were at least two orders of magnitude lower than sample intensities for the studied elements.

### 2.4. Reporting

REY patterns in the bulk rocks are shown as REY<sub>CN</sub> patterns (REY concentrations normalized to C1 chondrite of Anders and Grevesse (1989)). REY patterns in leachates are shown as REY<sub>BN</sub> patterns (REY concentrations normalized to those of the respective bulk rock). We emphasize that because neither chondrite nor any of the bulk rocks display Ce anomalies, the presence or absence of Ce anomalies in the leaching solutions is not affected by the type of reference material used for normalization.

The Ce/Ce\* ratio is a measure of the anomalous behavior of Ce and quantifies a Ce anomaly; values below unity

Table 2

Bulk rock trace element compositions (in mg/kg) of the rock samples used for the leaching experiments in this study. OIB = Ocean Island Basalt; MORB = Mid-Ocean Ridge Basalt.

Sample ID	OIB-Me	OIB-Haw	MORB-EPR	EPR <sub>glass</sub>	MORB-TP	TP <sub>glass</sub>	A-Jp	OL20B	GSAF3
Locality	Mehetia Island	Kilauea, Hawaii	East Pacific Rise		Turtle Pit		Hokkaido, Japan	Transvaal, South Africa	Bushveld, South Africa
Rock type	Alkali basalt	Tholeiitic basalt	Microcryst. basalt	Basalt glass	Microcryst. basalt	Basalt glass	Island-arc andesite	Basaltic andesite	Granite
mg/kg									
La	41.15	11.47	3.44	3.44	2.92	2.96	4.55	19.10	67.36
Ce	89.60	28.56	11.60	11.70	8.69	8.87	10.50	37.60	147.35
Pr	11.45	4.18	2.12	2.15	1.48	1.51	1.48	4.32	17.61
Nd	48.87	19.85	12.10	12.10	8.1	8.19	6.86	16.80	60.16
Sm	10.52	5.28	4.35	4.34	2.77	2.83	1.87	3.35	16.44
Eu	3.23	1.86	1.51	1.53	1.08	1.1	0.68	1.01	0.38
Gd	9.46	5.75	6.00	6.08	3.86	3.88	2.26	3.25	18.79
Tb	1.29	0.88	1.07	1.09	0.671	0.68	0.37	0.51	3.73
Dy	6.43	5.16	7.32	7.27	4.49	4.61	2.46	3.16	26.25
Y	27	24.26	40.7	41.1	25.8	26.1	13.94	18.0	160.7
Ho	1.06	0.97	1.58	1.56	0.963	0.98	0.54	0.67	5.41
Er	2.49	2.54	4.62	4.65	2.81	2.86	1.56	1.93	16.43
Tm	0.29	0.33	0.66	0.66	0.4	0.41	0.22	0.28	2.15
Yb	1.59	1.97	4.28	4.27	2.58	2.64	1.56	1.88	15.64
Lu	0.22	0.29	0.66	0.65	0.392	0.391	0.23	0.29	2.22
Th	6.69	0.88	0.14	0.14	0.147	0.157	0.91	5.45	66.97
U	1.83	0.30	0.07	0.07	0.051	0.056	0.31	1.67	21.1
Zr	317	145.2	119.7	119.4	80.1	81.2	40.91	100.10	349
Hf	7.30	3.90	3.26	3.30	2.0	2.03	1.25	2.56	14.71
Ce/Ce*	0.95	0.99	1.12	1.13	1.06	1.06	0.95	0.92	0.98
Y/Ho	25.47	24.91	25.76	26.35	26.79	26.63	25.83	26.91	29.7
Th/U	3.7	2.9	2.0	1.9	2.9	2.8	3.0	3.3	3.2
Zr/Hf	43.4	37.2	36.7	36.2	40.1	40.0	32.7	39.1	23.7

represent negative and values above unity positive Ce anomalies. The Ce/Ce\* ratio is calculated after [Bau and Dulski \(1996a\)](#) from normalized data as:

$$\text{Ce/Ce}^* = \frac{\text{Ce}_{\text{CN}}}{\text{La}_{\text{CN}}^{0.67} * \text{Pr}_{\text{CN}}^{0.33}} \quad (1)$$

### 3. RESULTS

#### 3.1. Bulk samples

The trace element composition of the bulk rocks is listed in [Table 2](#). Our measurements confirm previously published data within analytical uncertainty ([Binard et al., 1993](#); [Giese and Bau, 1994](#)). The REY<sub>CN</sub> patterns of all MORB samples ([Fig. 2a](#)) show depletion of the light REY (LREY; La–Sm) relative to the middle REY (MREY; Sm–Dy) and are flat between MREY and heavy REY (HREY; Gd–Lu). Such a REY distribution is typical of N-type MORB (e.g., [Hémond et al., 2006](#)). There is no difference between the crystalline MORB and the respective MORB glass. The OIBs ([Fig. 2a](#)) show LREY-enriched REY<sub>CN</sub> patterns without any Eu anomaly. The REE<sub>CN</sub> patterns of the andesitic rocks and the granite ([Fig. 2b](#)) decrease (steeply for the basaltic andesite and the granite) from the LREY to the MREY and are almost flat from the MREY to the HREY. None of the samples except for

the granite shows a Eu anomaly, and, notably, no sample shows any Ce anomaly.

The Zr/Hf ratios (32–45; [Table 2](#)) of the bulk rocks (except for the granite) are chondritic to slightly higher and indicate CHARAC trace element behavior. The granite, however, shows a sub-chondritic Zr/Hf ratio of 23.7. Thorium and U concentrations are positively correlated and plot on a straight line defined by the chondritic and the average upper continental crustal Th/U ratio ([Fig. 7](#)).

#### 3.2. Leachates

##### 3.2.1. Rare earth elements and yttrium

Trace element data for the leaching solutions are reported in [Table 3](#) and their REY<sub>BN</sub> patterns are shown in [Fig. 3a](#) and b. The REY<sub>BN</sub> patterns for the basalt leachates with DFOB are flat between the MREY and the HREY and show either a (small) negative Eu anomaly ([Fig. 3a](#): MORB-EPR, MORB-TP, OIB-Haw, OIB-Me; [Fig. 3b](#): A-JP, OL20B, GSAF3) or no Eu anomaly ([Fig. 3a](#): MORB-TP<sub>glass</sub>, MORB-EPR<sub>glass</sub>). The LREY distribution is more variable, but La and Pr are always depleted relative to the other REY. The REY<sub>BN</sub> patterns of the leachates with DFOB of the more evolved igneous rocks are more diverse with slightly decreasing, flat and slightly increasing patterns between the MREY and HREY ([Fig. 3b](#)). While La is the most strongly depleted

Table 3

Trace element compositions of the siderophile-bearing leachates after a leaching time of 24 h. Concentrations given are ng/kg. Final pH for replicate experiments shown in parentheses.

Sample ID	OIB-Me	OIB-Haw	MORB-EPR	MORB-EPR <sub>glass</sub>	MORB-TP	MORB-TP <sub>glass</sub>	A-Jp	OL20B	GSAF3
ng/kg									
La	458	169	112	3.5	202	54.8	139	73.8	3046
Ce	11439	3336	4919	367	2493	381	3993	1620	56563
Pr	610	299	394	19.9	287	52.3	268	104	4552
Nd	3071	1460	2540	170	1477	252	1458	576	22564
Sm	893	419	1213	128	498	82.4	550	167	9899
Eu	228	109	242	48.3	126	32.1	97.3	35.8	215
Gd	800	452	1652	199	664	115	651	185	12935
Tb	105	64.8	282	35.5	108	19	99.2	32.9	2564
Dy	601	380	1984	260	755	132	650	207	15860
Y	2356	1810	11171	1482	4461	3828	3661	1350	65160
Ho	94.1	72.1	429	54.1	151	27.3	130	45.9	2731
Er	220	192	1253	152	464	81.6	378	142	6624
Tm	23.7	22.9	155	20.4	63.9	10.4	47.7	18.8	739
Yb	151	150	1214	155	444	75	337	139	4127
Lu	17.9	21	179	21.8	62.3	11.1	52	21.9	478
Th	719	86.2	70.5	7.7	75.8	25.3	113.1	20.2	7814
U	265	41.2	87.1	45.5	37.4	9.6	90.6	131	32597
Zr	8223	4113	20397	1425	7226	943	3114	3270	10368
Hf	135	71.2	364	27.1	122	17.3	68.2	78.3	366.9
Ce/Ce*	6.31	4.53	8.02	16.00	3.04	1.95	6.41	5.41	4.54
Y/Ho	25.04	25.09	26.06	27.37	29.51	140.10	28.07	29.41	23.85
Th/U	2.71	2.09	0.81	0.17	2.03	2.64	1.25	0.15	0.2
Zr/Hf	60.7	57.7	56.0	52.5	59.4	54.4	45.7	41.8	28.3
pH start	5.5	5.5	5.5	5.5	5.5	5.5	5.5	5.5	5.5
pH end	8	7.69	8.4 (8.3)	8.2 (8.2)	8.8 (8.7)	8.5 (8.3)	7.43	8.45	7.82

REY in the leachates, all leaching solutions with DFOB show a positive Ce anomaly (Figs. 3 and 4). In the presence of DFOB, Ce and La show this behavior regardless of the pH during the leaching experiment and irrespective of the rock type, the rock texture (crystallinity, grain size), and the mineralogical or chemical composition of the leached material. The concentration of Fe which is the most important competitor of the REY (and HFSE) for the DFOB complexing ligand, obviously does also not exert a strong control on the behavior of the REY (and HFSE) during water–rock interaction in the presence of DFOB, as is suggested by the similar general trace element distribution in the leachates of Fe-rich basalts and of Fe-poor granite (Figs. 3 and 4).

Fig. 4a illustrates the difference between REY mobilization from andesite (OL20B) during leaching with 1 mM DFOB, with 1 mM HCl and 1 mM acetic acid, respectively. The REY<sub>BN</sub> patterns of the leachates are normalized to Yb to emphasize differences in REY fractionation caused by the different reagents. Mobilization of the HREY was more effective in the presence of DFOB, and La-depleted LREY-concave patterns with positive Ce anomalies in the leaching solutions only developed in the presence of DFOB. Fig. 4b shows the REY<sub>BN</sub> patterns of all DFOB leachates normalized to Yb to simplify comparison of the REY patterns. We emphasize that only leaching in the presence of the DFOB siderophile produces solutions that are significantly depleted in La and anomalously enriched in Ce relative to the respective bulk rock.

### 3.2.2. High field strength elements (Zr, Hf, Th, U) and Zr/Hf and Y/Ho ratios

Considerable amounts of Zr, Hf, Th and U are present in all leachates. Their concentrations range from 943 to 10,368 ng/kg for Zr, 17.3 to 367 ng/kg for Hf, 7.7 to 7813 ng/kg for Th and 9.6 to 32,597 ng/kg for U. Yttrium and Ho concentrations in the leachates are 1350–65,160 ng/kg and 27.3–2731.2 ng/kg, respectively. For all investigated elements, the granite leachate shows the highest HFSE concentrations whereas the leachates of the basaltic volcanic glasses show the lowest HFSE concentrations (see Table 3).

Figs. 5 and 6 show graphs of Zr/Hf ratios vs. Y/Ho ratios and Ce anomalies (i.e., Ce/Ce\* ratios) vs. Th/U ratios, respectively, of the bulk rocks and the corresponding siderophile leachates. Both geochemical twin pairs, Y–Ho and Zr–Hf, fractionate only slightly during leaching and their ratios differ only slightly from those in the respective bulk rock (Fig. 5). All MORB, OIB and andesite leachates are enriched in Zr over Hf relative to bulk rock, indicating minor incongruent solubilization and fractionation of Zr from Hf with preferential mobilization of Zr in the presence of siderophores. Except for the leachates of the OIBs (OIB-Me, OIB-Haw) and the granite (GSAF3), all leachates are enriched in Y over Ho, i.e., have slightly higher Y/Ho ratios than the corresponding bulk rock. The leachate of the granite is enriched in Ho over Y (relative to bulk rock), and Y–Ho fractionation is insignificant in the leachates of the OIBs.

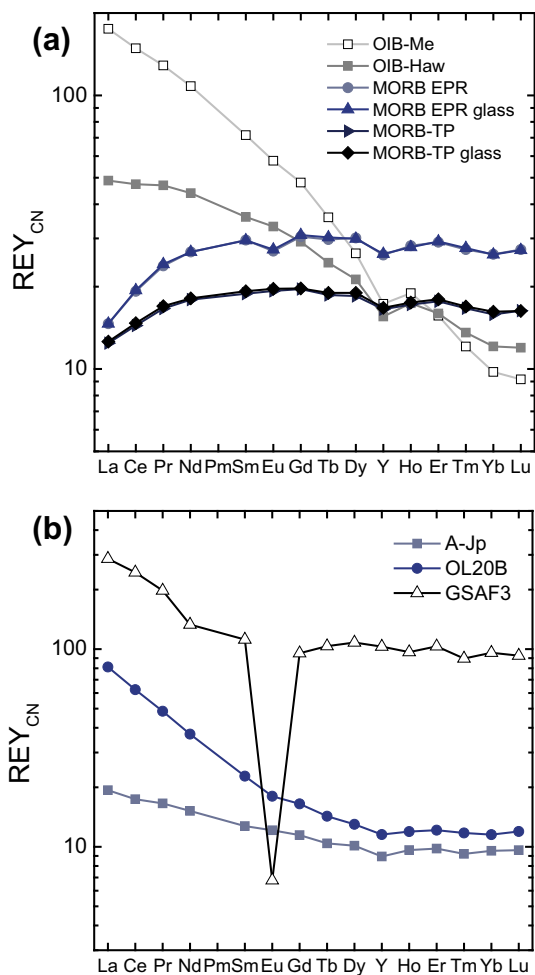


Fig. 2. Chondrite-normalized REY patterns of (a) ocean island basalts and mid-ocean ridge basalts, and (b) the two andesites A-Jp and OL20B and the Bushveld granite GSAF3 used in the leaching experiments. Bulk rock concentrations are provided in Table 2. Chondrite after Anders and Grevesse (1989).

In the presence of the DFOB siderophore, all leachates show a Ce/Ce\* ratio above unity, i.e., a positive Ce anomaly (Fig. 6). The Th/U ratios of all leachates are, except for the MORB-TP<sub>glass</sub> leachate, below the respective bulk rock ratio, i.e., the leachates are significantly enriched in U over Th relative to the bulk rocks (Fig. 7). The leachates of the andesite and the OIBs have slightly higher Ce/Ce\* ratios than the other leachates. Regardless of the rock type, the rock texture and the mineralogical or chemical composition, all leachates show fractionated Th/U ratios due to preferential U enrichment, and elevated Ce/Ce\* ratios, i.e., preferential Ce enrichment relative to the other REE, suggesting that both U and Ce might be mobilized by a similar mechanism.

Mobilization of Y, Ho, Zr, Hf, Th and U in the presence of DFOB is significantly more pronounced from the crystalline MORB than from the respective volcanic glasses (Fig. 8a). The MORBs show preferred mobilization of Th and U over Zr, Hf, Y and Ho. Zirconium, Hf, Y and Ho are virtually unfractionated. Control experiments without DFOB (plain DI) had concentrations of these trace elements that were below the determination limit of the

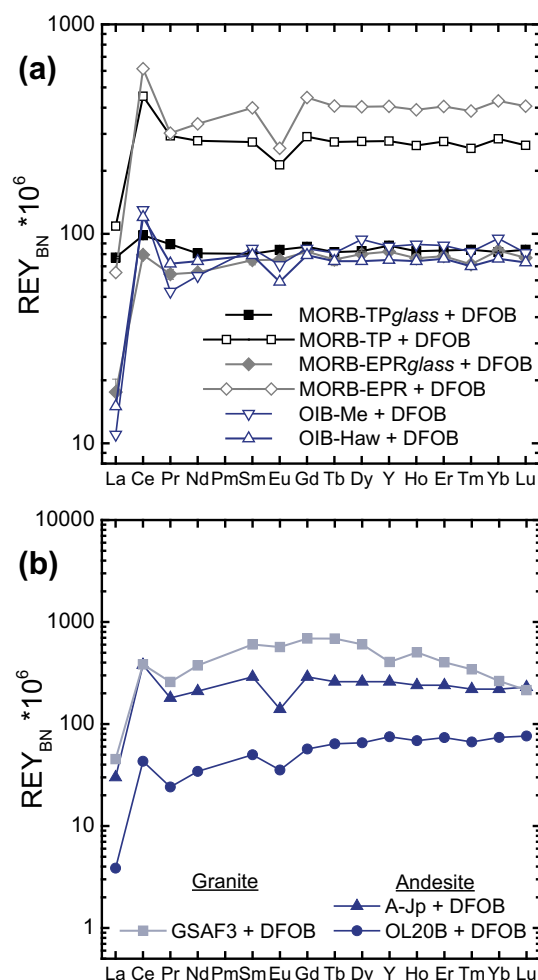


Fig. 3. Bulk rock-normalized REY patterns of leachates from experiments conducted on (a) mid-ocean ridge basalts (MORB) and ocean island basalts (OIB), and (b) on granite and (basaltic) andesites.

analytical technique applied, i.e., at least two orders of magnitude lower than the DFOB-bearing solutions.

Yttrium and Ho are enriched in the OIB and andesite leachates relative to Zr, Hf and Th (Fig. 8b). Zirconium, Hf and Th exhibit an upward pattern toward U in the siderophore leachates (Fig. 8a and b) for MORBs, OIBs and andesites. U is significantly enriched relative to other HFSEs in all leaching experiments, except for the MORB-TP<sub>glass</sub>.

We emphasize that similar types of rocks (e.g., the two OIBs or the four MORBs) demonstrate very similar trace element mobilization behavior when leached with siderophores. Hence, the Th–U and Y–Ho fractionation is specific for the interacting rock–siderophore system.

## 4. DISCUSSION

### 4.1. REY(III) mobilization with siderophores

The REY are traditionally assumed to be largely immobile during water–rock interaction (e.g., Bau, 1991). While

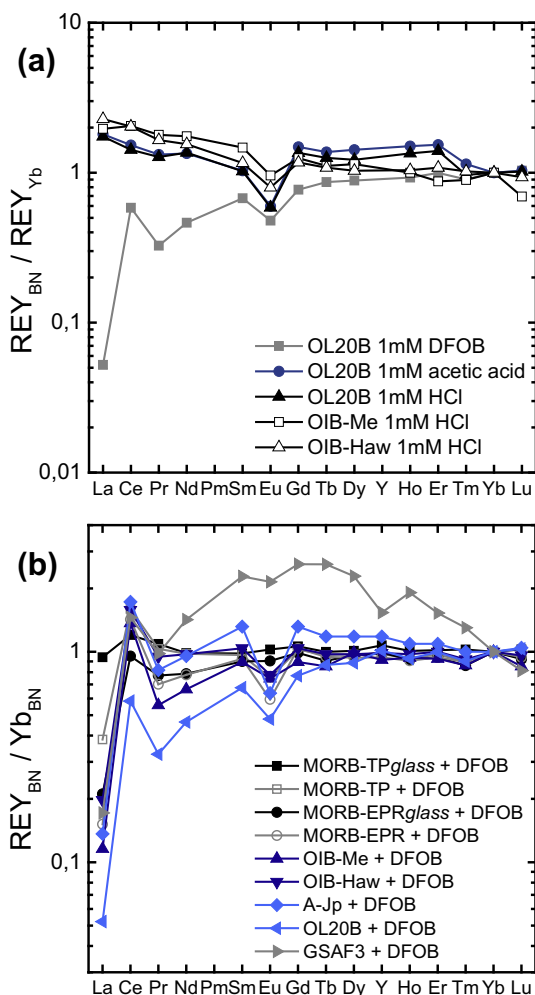


Fig. 4. Yb-normalized bulk rock-normalized REY patterns of leachates from experiments conducted on (a) andesite sample OL20B with 1 mM DFOB, 1 mM acetic acid and 1 mM HCl, and on OIB-Me and OIB-Haw with 1 mM HCl, and (b) various rock types with DFOB-bearing solutions. Note in (a) that neither HCl nor acetic acid produces the LREY-concave patterns and the positive Ce anomaly that are typical of leaching in presence of DFOB. Only in the presence of the DFOB siderophore does leaching produce solutions with positive  $Ce_{BN}$  anomaly and La-depleted concave -downward LREY patterns (b). All leachates show negative  $Eu_{BN}$  anomalies except for those from the MORB glasses.

varying concentrations of complexing ligands, pH and other environmental parameters are likely to influence leaching efficiency, the more than 100-fold enrichment of the REY in the DFOB-bearing solutions relative to the DFOB-free ones suggests that siderophores have a very profound impact on REY mobility. This may affect REY mobilization in a variety of natural environments and processes, such as continental weathering and pedogenesis, diagenetic water–rock interaction in unconsolidated sediments, and particle-dissolution in seawater and in freshwater systems. Mobility of REY in supergene environments may offer opportunities for (bio)geochemical resource exploration, but may also increase their bioavailability and their potential for environmental contamination.

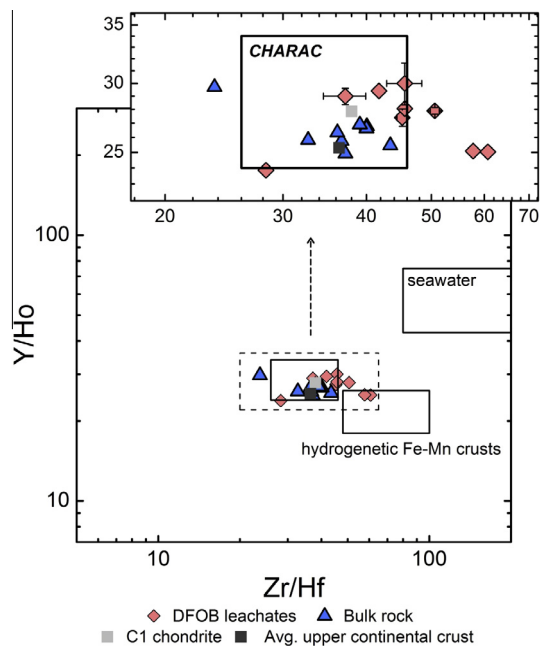


Fig. 5. Graph of Zr/Hf ratio vs. Y/Ho ratio for bulk rocks and their leachates from batch leaching experiments with powdered igneous rocks. Open symbols represent leachates, while bulk rock ratios are shown in solid symbols. Note that fractionation of both geochemical twin pairs, Y–Ho and Zr–Hf, is only small. Replicate experiments (error bars) for the leachates indicate a good reproducibility of the experimental data. C1 chondrite and average continental crust data from Anders and Grevesse (1989) and Rudnick and Gao (2003), respectively. CHARAC-, seawater- and hydrogenetic Fe–Mn crust arrays from Bau (1996) and Schmidt et al. (2014).

The different mineralogical compositions and textures of the samples studied and the different pH conditions during the individual batch leaching experiments led to markedly different absolute trace element concentrations in the leachates. However, the Yb-normalized  $REY_{BN}$  patterns (Fig. 4b) reveal the general fractionation trend within the REY group and highlight differences between the type of fractionation imposed by the specific chelators present in the different leaching solutions.

Without any exceptions and independent of pH, leaching of volcanic rocks in the presence of DFOB produced  $REY_{BN}$  patterns in the leachate that show depletion of the LREY relative to the middle and heavy REY (Fig. 3a and b) and concave downward LREY patterns. This depletion is most pronounced for La and becomes smaller with increasing LREY atomic number. This feature is neither produced during leaching with DI water, nor with HCl or acetic acid (Fig. 4a).

Negative Eu anomalies in leaching solutions of mafic, intermediate and felsic igneous rocks have been suggested to be the ultimate result of the preferential incorporation of Eu into feldspars (Giese and Bau, 1994; Bach and Irber, 1998; Bau et al., 1998; Shibata et al., 2006). In basalts and basaltic andesites, the melt in the vicinity of a growing plagioclase crystal becomes selectively depleted in Eu due to preferential partitioning of  $Eu^{2+}$  into the crystal lattice of

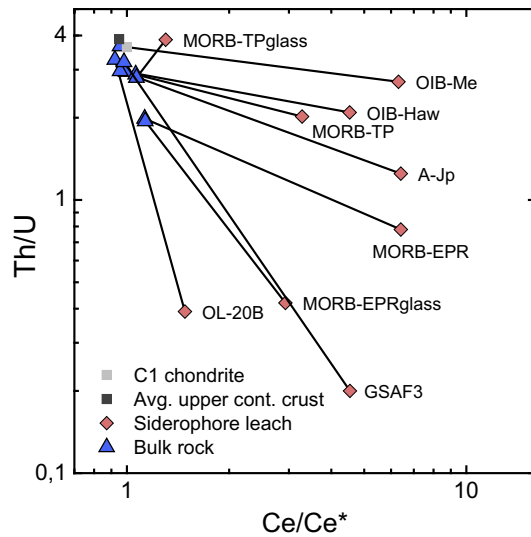


Fig. 6. Graph of Ce anomaly (expressed as  $Ce/Ce^*$ ) vs. Th/U ratio of bulk rocks and the respective leachates. Note that all leachates show positive Ce anomalies (i.e.,  $Ce/Ce^* > 1$ ) and that Th/U ratios are strongly fractionated. The exceptional Th/U ratio for the MORB-TPglass leachate was verified in three replicate experiments. C1 chondrite and average continental crust data from Anders and Grevesse (1989) and Rudnick and Gao (2003), respectively.

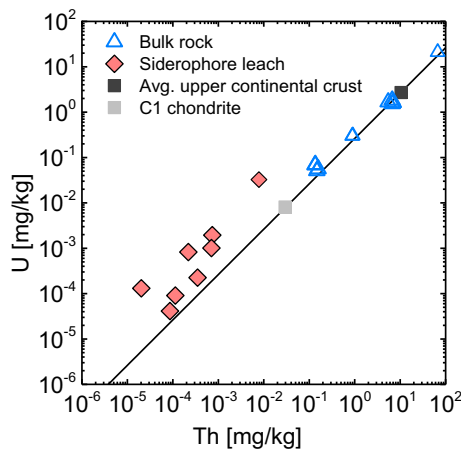


Fig. 7. Graph of Th vs. U concentration for leachates and corresponding bulk rocks. While Th and U are positively correlated in the bulk rocks ( $R^2 = 0.99$ ), all leachates are strongly enriched in U over Th relative to their respective bulk rock, and fall above the trend line of  $Th/U = 3.8$ , defined by chondrite and average upper continental crust. C1 chondrite and average continental crust data from Anders and Grevesse (1989) and Rudnick and Gao (2003), respectively.

plagioclase, leading to REY patterns with negative Eu anomalies at grain boundaries, in the groundmass and in the interstitial space between crystals (Giese and Bau, 1994). Because feldspars and other rock-forming minerals do not readily dissolve during short-lived water–rock interaction, it is the easily accessible REY load of this Eu-depleted pool in grain boundaries, ground mass and

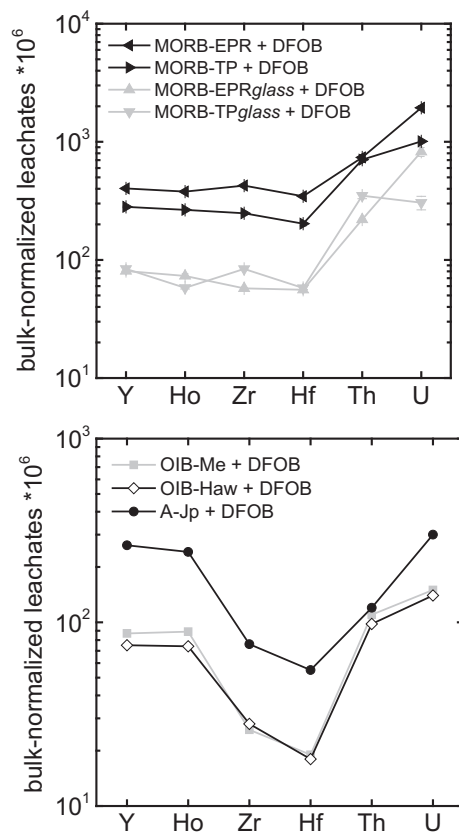


Fig. 8. Bulk rock-normalized trace element patterns for leachates from (a) microcrystalline basalts (MORB-EPR and -TP) and their corresponding glassy counterparts (EPRglass and TPglass, respectively), and of the ocean island basalts OIB-Me and -Haw and the island-arc andesite A-Jp (b). Note that error bars obtained by two replicate experiments are smaller than the symbols for all elements except for U in (a).

interstitial space, that is preferentially mobilized, producing leachates with negative  $Eu_{BN}$  anomaly (Giese and Bau, 1994; Bau et al., 1998). Thus, leaching of rocks without a significant feldspar component, such as basaltic glass, should not produce leaching solutions with a negative  $Eu_{BN}$  anomaly. Our experimental results fully support this hypothesis (Fig. 3a and b): both MORB glasses produce leachates without any negative  $Eu_{BN}$  anomaly and the glass-rich sample OIB-Me shows only a very small one (Fig. 3a).

Europium anomalies in granites result from trace element partitioning between minerals and melt during fractional crystallization and, more importantly, partial melting, as lower crustal partial melts are depleted in Eu due to the presence of Eu-enriched feldspar in the residuum (e.g., Taylor and McLennan, 1985). Hence, the  $REY_{CN}$  pattern of the granite GSAF3 shows a large negative Eu anomaly (Fig. 2b). However, the  $REY_{BN}$  pattern of the granite leachate does not show a Eu anomaly (Fig. 3b), revealing that Eu is not decoupled from its REY neighbors during the 24 h granite leaching experiment.

The strong depletion of La relative to the other LREY in the basalt leachates might on first sight suggest

decoupling of La from the other LREY. Such partial decoupling and the subsequent formation of La anomalies are known from seawater and from some chemical sediments, and have been observed during REY scavenging by Fe and Mn (hydr)oxides (Bau and Dulski, 1996b; Bau, 1999; Bau and Koschinsky, 2009). Lanthanum-LREY decoupling has been explained by anomalously low hydrolysis constants of La as compared to its LREY neighbors, which ultimately results in positive La anomalies in the aqueous phase and negative La anomalies in the solid (e.g., Bau, 1999). However, in such cases the La anomaly is usually accompanied by Gd anomalies and strong Y–Ho fractionation or even lanthanide tetrad effects (Bau, 1996, 1997, 1999), which we did not observe in our experiments. Rather, leaching with DFOB in general produces solutions whose REY<sub>BN</sub> patterns are concave between La and Sm and which increase smoothly and systematically from La to the MREY. Because this is observed for leaching of both crystalline and glassy EPR basalt, it can be ruled out that this REY signature is the result of a mineralogical control during REY mobilization, but rather demonstrates that this signature develops specifically during leaching in the presence of DFOB.

A full set of stability constants for REY-DFOB complexes (Fig. 1) is available for the trivalent REY at seawater ionic strength of 0.7 (Christenson and Schijf, 2011). This high-quality data set indicates that the stability constants of the bi-, tetra- and hexadentate REE(III)-DFOB complexes increase most sharply from La to Sm. This relationship compares favorably with the REY<sub>BN</sub> patterns observed in our leachates, which show only little fractionation between the MREY and HREY, but more pronounced fractionation between La and the MREY (Fig. 3a and b). This indicates that the presence of the DFOB siderophore preferentially promotes the mobilization of MREY<sup>3+</sup> and HREY<sup>3+</sup> over that of LREY<sup>3+</sup>, and that La is the REY which is least affected by siderophore-promoted REY mobilization.

#### 4.2. Oxidative mobilization of cerium

Cerium is the only REY that in natural low-temperature environments can occur in two oxidation states (+3 and +4). While Ce<sup>3+</sup> behaves similarly to its strictly trivalent REY neighbors, Ce<sup>4+</sup> shows significantly different behavior during geochemical processes because of different partition coefficients, solubilities and complex stabilities of Ce(IV) as compared to Ce(III) and its respective compounds. This leads to a decoupling of tetravalent Ce from its trivalent REY neighbors and causes the formation of Ce anomalies in normalized REY patterns. Although the inorganic chemical oxidation of Ce<sup>3+</sup> is slow, surface catalysis and microbial mediation may promote Ce<sup>3+</sup> oxidation (e.g., Moffett, 1990) and subsequent formation of Ce anomalies in low-temperature environments (Bau, 1999; Ohta and Kawabe, 2001; Yoshida et al., 2004; Davranche et al., 2005, 2008; Bau and Koschinsky, 2009; Tanaka et al., 2010). Negative Ce anomalies are common in oxic waters because of oxidative scavenging of Ce on particle surfaces and/or Ce fixation due to formation of insoluble Ce(IV)

compounds (e.g., Bau and Koschinsky, 2009; Bau et al., 2014 and references therein). The only known exception is the CO<sub>3</sub><sup>2-</sup>-rich waters of some alkaline lakes which show positive Ce anomalies (Möller and Bau, 1993; Johannesson and Lyons, 1994; Johannesson et al., 1994) due to the stabilization of Ce(IV) polycarbonate complexes in solution (Möller and Bau, 1993). Preferential stabilization of dissolved Ce(IV) compounds has also been observed in experimental studies of competitive complexation of REY by humic acids and CO<sub>3</sub><sup>2-</sup> (Pourret et al., 2007). Similar to the situation in alkaline lakes, however, Pourret et al. (2007) argue that Ce<sup>3+</sup> oxidation is promoted by the formation of Ce(IV) pentacarbonate complexes and that only in a second step is Ce(IV) bound to the humates. Because humates are a substantial part of the colloidal REY fraction in organic matter-rich natural waters, this does not produce a positive Ce anomaly in the truly dissolved REY fraction, but in the nanoparticulate and colloidal REY fraction in the water.

As shown by our experiments (Figs. 3 and 4), leaching of volcanic rocks in the presence of DFOB typically produces solutions with a positive Ce anomaly. The behavior of Ce(III) in presence of DFOB should be similar to its LREY neighbors due to the fact that Ce<sup>3+</sup> has the same ionic charge and a comparable ionic radius. Therefore, no fractionation of Ce from its neighbors is to be expected unless Ce<sup>3+</sup> is oxidized. Several studies (e.g., Hernlem et al., 1999; Duckworth et al., 2009, 2014; Kraemer et al., 2014) demonstrated that the stability constant of a metal with DFOB is positively correlated to its ionic potential (charge to radius ratio). This relation suggests, that Ce(IV)-DFOB complexes should be as stable as Fe(III)-DFOB complexes (Fig. 9), thus facilitating significant decoupling of Ce from its LREY neighbors.

The selective decoupling of Ce from the other REY in our experiments with DFOB demonstrates that Ce<sup>3+</sup> is oxidized during its solubilization during water–rock interaction. The preferential mobilization of Ce is confined to leaching in the presence of DFOB, regardless of the prevailing pH, and regardless of the type, texture and mineralogical or chemical composition of the rock that is leached. This suggests the formation of a Ce(IV) DFOB complex that is significantly more stable than its Ce(III) counterpart, as suggested in Fig. 9. This interpretation is supported by previous observations that Ce shows anomalously low adsorption on bacterial cells (relative to the other REY) in the presence of DFOB (Yoshida et al., 2004; Ozaki et al., 2006). Trivalent Ce was oxidized during these adsorption experiments and rapidly bound in a highly stable Ce(IV) DFOB complex in solution (Yoshida et al., 2004; Ohnuki et al., 2005). Bau et al. (2013) indicated that Ce(III) is probably oxidatively solubilized when melt- and riverwater rich in mafic volcanic ash is incubated with the DFOB siderophore. Our experimental results reveal that this process is not limited to volcanic ash in river water, but also affects igneous rocks when these are leached with siderophore-containing solutions. This suggests that HFSE and REY are preferentially mobilized from rocks, whenever siderophores like DFOB are present in natural weathering solutions. Our results also corroborate the

hypothesis that the preferential release of Ce observed during microbial leaching of artificial hornblende glass (Brantley et al., 2001) resulted from the excretion of siderophores by bacteria and not from changes in pH or by the presence of other low-molecular weight organic acids.

Our results demonstrate that the formation of Ce(IV) polycarbonate complexes is not the only complexation mechanism that can promote fractionation of Ce from its REY neighbors. Siderophores like DFOB significantly enhance the solubility of Ce(IV) and can produce positive Ce anomalies in natural waters. While the formation of Ce(IV) pentacarbonate complexes requires high  $\text{CO}_3^{2-}$  activity and hence only operates in alkaline environments, complexation by siderophores can occur under mildly alkaline, near neutral and even mildly acidic conditions. This suggests that siderophore complexation can significantly impact Ce behavior and may cause Ce-REY decoupling in a much wider range of natural environments, including soil solutions, groundwaters, river and lake waters, seawater and marine porewaters.

#### 4.3. Mobilization and fractionation of Zr, Hf, Th and U by siderophores

High field strength elements such as Zr, Hf, Th, U and the REY hydrolyze easily and are particle-reactive, i.e., they readily bind to hydroxyl and carboxyl groups, for example, on particle surfaces. As a result, truly dissolved concentrations of these HFSE in natural waters are usually very low, due to their immediate precipitation or sorption onto Mn or Fe (oxyhydr)oxides, clay minerals or organic particles, and there is general consent that in most geological settings HFSE are rather immobile during water–rock interaction (e.g., Jiang et al., 2005; Tepe and Bau, 2014, and references therein). In all of our experiments, the presence of

siderophores during leaching significantly enhanced the mobilization of the ‘immobile’ HFSE Zr, Hf, Th, U, and REY into the dissolved pool. The granite leachates yield the highest HFSE concentrations due to the higher abundance of these metals in the original rocks. The batch leaching experiments on crystalline MORB and MORB glasses demonstrate that all studied HFSE (including the REY) are more effectively mobilized from crystalline volcanic rock than from volcanic glass. In igneous rocks, the HFSE and REY are incompatible and usually are not incorporated into the crystal lattice of the major rock-forming minerals. Rather, they are enriched in interstitial spaces and in the ground mass of igneous rocks (Giese and Bau, 1994; Bau et al., 1998). This ‘loose’ bonding leads to an easy availability during leaching. Similar to previous results (Giese and Bau, 1994; Bau et al., 1998), our experimental results demonstrate that the HFSE and the REY are more readily leached by siderophores when these elements are located along grain boundaries and in a rock’s matrix.

Considering the stability constants of their various chemical complexes (Martell and Smith, 2001), siderophores do not only mobilize iron, but they should also be able to mobilize a wide range of HFSE (Fig. 9). This is in general agreement with the results of our leaching experiments, as in all these experiments we observed enhanced HFSE mobilization in the presence of siderophores, although with only minor fractionation of the geochemical twin pairs Zr–Hf and Y–Ho, but with strong Th–U fractionation due to preferential mobilization of U.

In all experiments, Th and U are more effectively mobilized than Zr, Hf, Y, and Ho. Comparing Th and U, U is preferentially mobilized and the leachates are strongly fractionated toward Th/U ratios that are lower than those of the respective bulk rocks. It is well known that DFOB

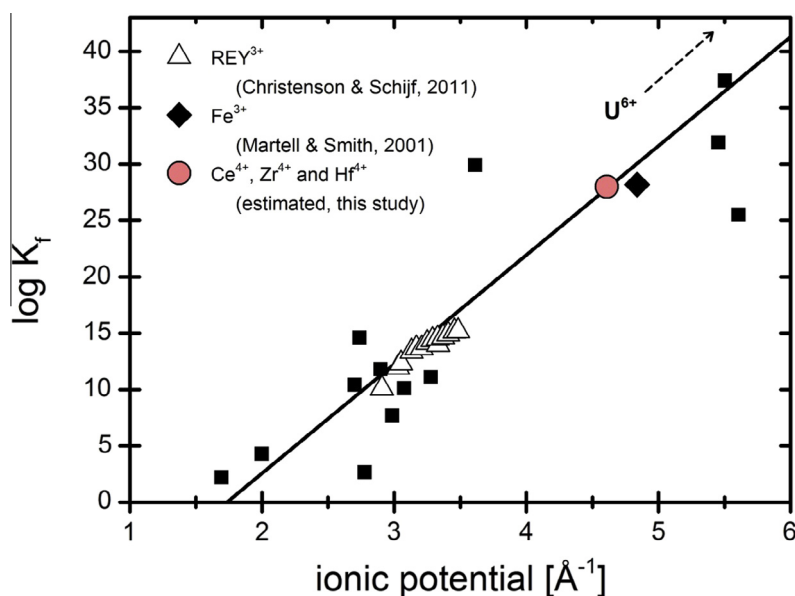


Fig. 9. Relationship between ionic potential and stability constants for metal complexes of  $\text{M}^{n+}\text{HDFOB}_2^{-n}$  adapted from Kraemer et al. (2014). Stability constants ( $\text{Fe}^{3+}$  and other  $\text{M}^{n+}$ ) taken from Martell and Smith (2001),  $\text{REY}^{3+}$  data from Christenson and Schjif (2011). Ce(IV)-, Zr(IV)- and Hf(IV)-complexes with DFOB are estimated using the regression line, suggesting them to be as stable as DFOB complexes with  $\text{Fe}^{3+}$ . Estimated U(VI)-DFOB complex stability constants are as high as  $\log K_f \gg 50$ .

forms stable complexes with U (Mullen et al., 2007; Wolff-Boenisch and Traina, 2007; Desouky et al., 2011 and others). We showed that leaching in the presence of DFOB not only enhances the dissolved concentrations of U in the leaching solutions, but that it also strongly promotes decoupling of U from Th.

Considering that in the presence of siderophores, redox-sensitive U behaves similar to redox-sensitive Ce (both are preferentially mobilized relative to redox-insensitive Th and LREY, respectively; Fig. 6), it is likely that this is due to the formation of a U(VI) DFOB complex in the leachate. The stability constant of DFOB with Th(IV) is reported by Martell and Smith (2001) to be in the range of  $\log K_f = 15.7$ . Due to the same oxidation state and similar radius of Th(IV) and U(IV), U(IV) stability constants with DFOB can be assumed to be in the same range as those of the Th(IV) DFOB complex. Mullen et al. (2007) determined the stability constants of U(VI) in the form of the uranyl ion ( $\text{UO}_2^{2+}$ ) with DFOB and showed that the stability constants of U(VI) DFOB complexes ( $\log K_f$ : 17.12–22.93) are significantly higher than that of Th(IV) and, thus, likely also of the U(IV) DFOB complex. Hence, if U(IV) formed complexes with DFOB and was mobilized as a U(IV) DFOB complex, Th–U fractionation should only be minor. If, however, U was present as U(VI), then complexation with DFOB resulted in significant decoupling of U from Th. Considering the correlation between the stability of metal DFOB complexes and the metals' ionic potential (Fig. 9), U(VI) DFOB complex stability constants should be in the range of  $\log K_f \gg 50$ , facilitating pronounced decoupling of U from Th. The siderophore leachates show strong Th–U fractionation in almost all experiments, suggesting that a significant fraction of total U in the leachates occurred as U(VI) species. In natural systems, Th is exclusively present as a tetravalent ion and its mobility is very limited due to the formation of  $\text{Th}(\text{OH})_4$  which is characterized by low solubility (Choppin, 2006). At neutral to alkaline pH, U is mostly present in the surface environment as one of several water-soluble uranyl ( $\text{U}(\text{VI})\text{O}_2^{2+}$ ) carbonate species (Grenthe et al., 2004; Choppin, 2006). In our experiments U(VI) carbonate speciation is negligible, because DFOB concentrations are two orders of magnitude higher than total  $\text{CO}_2$  concentration (assumed to be in equilibrium with atmosphere) and because DFOB complexes with uranyl are several orders of magnitude more stable (Mullen et al., 2007) than the carbonate complexes commonly prevailing in low-temperature aqueous solutions (Grenthe et al., 2004; Choppin, 2006).

Y–Ho and Zr–Hf are both slightly fractionated during mobilization in the presence of DFOB. How strong this fractionation is appears to depend on the specific rock type that interacts with the siderophore. Christenson and Schijf (2011) give the stability constants,  $\log K_f$ , of Y and Ho with DFOB for hexadentate complexes as 13.98 and 14.13–14.53, respectively. The stability constants of these two elements with DFOB are thus rather similar, suggesting that fractionation of Y and Ho induced by DFOB complexation should be minor. This is in agreement with the rather small Y–Ho fractionation observed in our leaching experiments (Fig. 5).

Yoshida et al. (2007) suggested that the stability constant for the Hf(IV) DFOB complex is similar to that of the Fe(III) DFOB complex and, hence, should be in the range of  $\log K_f = 30.7$  for hexadentate complexes (Martell and Smith, 2001). No data are available for the Zr(IV) DFOB complex, but its stability constants should be in the same range as Hf(IV) DFOB stability constants (Fig. 9) if the regression statistics shown by Kraemer et al. (2014) is also valid for Zr and Hf. Our batch leaching experiments showed only minor Zr–Hf fractionation with Zr/Hf ratios in the leachates only slightly above the bulk rock ratios. The minor fractionation of the Zr–Hf twin pair toward super-chondritic ratios suggests that the stability of Zr(IV) DFOB complexes is probably very slightly higher than that of Hf(IV) DFOB complexes, given that the host minerals of these geochemical twins are the same. Both, the mobilization of Zr–Hf and Y–Ho in the presence of DFOB can thus be explained by published thermodynamic data as a function of the specific stability constants with the DFOB siderophore. The dissolved concentrations of Zr and Hf in the granite leachates are orders of magnitude higher than in the mafic and intermediate rock leachates (see Table 3). In evolved rocks, almost all of the Zr and Hf are hosted in the zircon structure. The observed strong release of Zr and Hf during leaching of granite in the presence of siderophores (see Table 3 and Fig. 5) may imply that siderophores mobilize Zr and Hf from zircons, a mineral which is usually regarded as very weathering resistant.

It has been suggested that Hf is removed from the dissolved pool when river water mixes with seawater in estuarine systems because of aggregation and sedimentation of particles (e.g., Bau and Koschinsky, 2006; Godfrey et al., 2008). Thus, the amount of Hf that actually enters seawater via fluvial pathways should be rather small (Bau and Koschinsky, 2006). Due to this Hf removal and the preferential scavenging of Hf relative to Zr onto particles (e.g., Bau and Alexander, 2009; Schmidt et al., 2014), modern seawater shows super-chondritic Zr/Hf ratios (Godfrey et al., 1996, 2008; Firdaus et al., 2011), i.e., seawater is enriched in Zr over Hf. However, Firdaus et al. (2011) indicated that terrigenous sources are important for the budget of Zr and Hf in seawater. Our experiments corroborate results of incubation experiments (Bau et al., 2013) and demonstrate that Zr and Hf are complexed and mobilized in the presence of the DFOB siderophore (Fig. 8a + b; Table 3). Considering that siderophore complexes are chemically stable over a wide range of pH and Eh conditions (Kraemer, 2004), the transport of Hf as a Hf(IV) siderophore complex might limit sorption to river particles and suppress removal of Hf (and Zr) from riverine and estuarine systems by coagulation and sedimentation. The formation of strong complexes with siderophores may effectively facilitate the transport of continental Hf via estuaries into the open ocean.

#### 4.4. Impact of siderophores on geochemical applications using Ce and U

Our experiments demonstrate that redox-sensitive Ce and U are oxidized and eventually decoupled from LREY

and Th, respectively, during leaching in the presence of siderophores. For both elements, the reduced redox-species (Ce(III) and U(IV), respectively) are released from minerals and rocks, and depending on the physico-chemical environment (e.g., oxygen fugacity, temperature, pH), the specific  $Ce_{aq}^{4+}/Ce_{aq}^{3+}$  and  $U_{aq}^{6+}/U_{aq}^{4+}$  redox equilibria are established. However, oxidized  $Ce_{aq}^{4+}$  and  $U_{aq}^{6+}$  are immediately bound and removed as Ce(IV) DFOB and U(VI) DFOB complexes and in the attempt to maintain the redox equilibria, additional  $Ce_{aq}^{4+}$  and  $U_{aq}^{6+}$  are produced. The overall effect of this “siderophore redox pump” is the preferential enrichment of dissolved Ce and U relative to dissolved LREY and Th, respectively.

This may have a profound impact on the use of Ce and U as paleo-redox-proxies. In most anoxic natural environments, Th and U are both tetravalent and considered ‘immobile’ due to their very low solubilities. Thus, these two elements are not fractionated from each other during their release from minerals and rocks because of their same oxidation state. However, ‘immobile’ U(IV) is oxidized to ‘mobile’ U(VI) in Earth’s (near-)surface systems during oxidative weathering of minerals and rocks (e.g., Collerson and Kamber, 1999). Soluble U(VI) compounds such as uranyl, ( $U(VI)O_2^{2+}$ ), therefore, predominate over less soluble U(IV) species (Wilkins et al., 2006) and hence, modern oxic seawater, for example, shows dissolved Th/U ratios below unity (e.g., Asmerom and Jacobsen, 1993). These low Th/U ratios are eventually transferred to marine chemical sediments which act as archives of the Th/U ratio of seawater. Therefore, coupled or decoupled Th–U behavior may be used as a paleo-redox-proxy for tracking the evolution of the redox level of a geochemical system such as the Earth’s atmosphere and oceans (e.g., Rosing and Frei, 2004; Bau and Alexander, 2009; Crowe et al., 2013). Similarly, presence or lack of Ce anomalies in chemical sediments and precipitates, and in paleosols and paleoweathering profiles is used as a paleo-redox proxy (e.g., German and Elderfield, 1990; Möller and Bau, 1993; Bau et al., 1996; Pattan et al., 2005).

However, our experimental results suggest that the presence of strong organic ligands such as siderophores is sufficient to promote oxidation and mobilization of U and Ce. Therefore, if there is ample reason to believe that significant amounts of siderophores or other strong ligands were present during the deposition of a studied rock, the use of proxies such as U and Ce might be severely hampered. Our result may also be important in the field of applied environmental science. Extensive research has been conducted on the long-term U removal from contaminated soils and waters by fixing aqueous U(VI) to insoluble U(IV) minerals via bacterial activity (see Newsome et al., 2014 and references therein). Ganesh et al. (1997), for example, found that multidentate complexation with organic ligands substantially lowers the rate of U(VI) reduction by sulfate-reducing and ferric iron-reducing bacteria. Such a ‘shielding effect’ might also be observed for the very stable U(VI)-DFOB complexes, and complexation of U(VI) with DFOB, therefore, might suppress microbially induced U reduction in the environment. This may have widespread implications for the (bio-) remediation of

U-contaminated sites near nuclear waste repositories, for example, or for microbial bioleaching of low-grade U ore deposits (Choi et al., 2005; Qiu et al., 2011). Desouky et al. (2011) present a method to bioleach Th–U concentrates with siderophores and show very promising results for Th and U extraction. However, given the stabilities of U and Th DFOB complexes (Mullen et al., 2007) in the environment and given that DFOB complexes are stable over a wide range of pH and Eh (Kraemer, 2004), a potential leakage may cause severe environmental damage and hamper remediation efforts due to very strong binding of Th and U to multidentate organic ligands like DFOB.

Stern et al. (2014) already showed that humic acid complexation plays a vital role in the speciation and mobility of Th, Hf and Zr in the environment. Our data suggest that siderophores are another group of organic molecules that may play an equally important role in the mobilization and fractionation of these and other HFSE.

## 5. CONCLUSIONS

We studied the mobilization of REY, Zr, Hf, Th and U from volcanic rocks in the presence of the siderophore desferrioxamine B (DFOB), to see how low-temperature water–rock interaction during weathering, pedogenesis, or partial dissolution of particles in seawater and freshwater may affect the behavior of these trace elements. Our results demonstrate that chemical complexation with the DFOB siderophore significantly enhances the mobility of these HFSE and leads to two distinct features in REY patterns, that develop independently of pH and regardless of the mineralogy, the iron content and the texture of the rock being leached: (i) all leaching solutions display a positive Ce anomaly, and (ii) all leachates are depleted in the LREY (especially La) relative to the other MREY with a concave downwards  $LREY_N$  pattern. These features do not develop in the absence of DFOB during leaching with de-ionized water, hydrochloric acid or acetic acid. Other features, such as a negative Eu anomaly, are related to mineralogy and texture and may also be produced during leaching in the presence of hydrochloric or acetic acid.

The positive Ce anomalies are evidence for siderophore-promoted oxidative mobilization of Ce during low-temperature water–rock interaction and indicate the formation of a very stable, water-soluble Ce(IV) DFOB complex. This Ce(IV) siderophore complex has the potential to create natural waters with positive Ce anomaly over a much wider pH range than Ce(IV) pentacarbonate complexes that are confined to  $CO_3^{2-}$ -rich alkaline environments. Weathering by siderophore-bearing solutions may thus produce Ce anomalies in environments that otherwise are too acidic and/or reducing to develop Ce anomalies, which further complicates the use of Ce anomalies as quantitative (paleo)redox proxies.

The fractionation and conspicuous shape of the REY pattern between the LREY and MREY is consistent with REY(III) DFOB stability constants (Christenson and Schijf, 2011) and the La-depleted concave downward LREY pattern could potentially be used as an indicator for the presence of biogenic chelators such as DFOB during

water–rock interaction. While it is clearly premature to use La-depleted concave downward LREY patterns as a siderophore-imposed biosignature, for example in Paleozoic or Proterozoic paleosols or (ancient) chemical sediments, this possibility warrants further study.

We also showed that the presence of siderophores also significantly enhances the concentrations of ‘immobile’ HFSE such as Zr, Hf, Th and U in aqueous solutions. Analogous to Ce, preferential mobilization of U is attributed to siderophore-induced oxidative solubilization. In the presence of DFOB, U is oxidized from U(IV) to U(VI), which may have widespread implications for the use of Th–U as a (paleo)redox proxy, because in the presence of the DFOB siderophore, U is more effectively mobilized than Th, leading to Th/U signals comparable to those indicative of weathering under oxidized conditions. Mobilization of the two geochemical twin pairs Y–Ho and Zr–Hf is characterized by ligand-promoted dissolution mechanisms and the mobilization with only minor fractionation observed in the leaching experiments appears to be a function of the specific metal-DFOB stability constant.

Our experiments showed that natural biogenic ligands such as siderophores are capable of solubilizing and complexing elements like the HFSE investigated here and, hence, facilitate the mobilization of ‘immobile’ trace elements during the weathering of rocks. Metal transport as siderophore-complexed compounds might represent an important pathway for the transport of (trace) elements (which may be (micro)nutrients or (micro)contaminants) from rocks and volcanic ashes to natural waters and to increase their bioavailability. Additionally, the transport of dissolved HFSE like Hf as siderophore complexes might efficiently alter their respective particle-reactivity and prevent their sorption onto particles during estuarine mixing processes. The enhanced mobilization of Zr and Hf from igneous rocks and volcanic ash particles might represent an important pathway for Hf from the continents into the oceans, which may have implications for the use of Hf isotopes as water mass tracers and as probe into continental weathering regimes.

Although DFOB concentrations in seawater samples are usually in the nanomolar range (e.g., Kraemer, 2004), DFOB concentrations can reach more than 0.13 mM in soil solutions (Watteau and Berthelin, 1994; Kraemer, 2004). Considering the wide range of siderophore compounds identified in natural systems (Boukhalfa and Crumbliss, 2002) it is most likely that oxidative mobilization of Ce and U as well as enhanced mobilization of other HFSE such as Zr and Hf, is not unique to desferrioxamine-B, but likely promoted by other natural siderophores as well. This suggests a significant impact of siderophores on trace element (re-)distribution during weathering of rocks and minerals.

#### ACKNOWLEDGEMENTS

We appreciate the help of D. Meissner and J. Mawick in the Geochemistry Lab at Jacobs University Bremen. We thank K. Wortberg for her assistance during the leaching experiments. The manuscript benefited from comments of GCA reviewer H. Buss,

University of Bristol, of an anonymous reviewer, and of GCA editor J. Chorover.

#### REFERENCES

- Akafia M. M., Harrington J. M., Bargar J. R. and Duckworth O. W. (2014) Metal oxyhydroxide dissolution as promoted by structurally diverse siderophores and oxalate. *Geochim. Cosmochim. Acta* **141**, 258–269.
- Albrecht-Gary A. M. and Crumbliss A. L. (1998) Coordination chemistry of siderophores: thermodynamics and kinetics of iron chelation and release. In *Metal Ions in Biological Systems* (eds. A. Sigel and H. Sigel). CRC Press, p. 824.
- Alexander B. W. (2008) Trace element analyses in geological materials using low resolution inductively coupled plasma mass spectrometry (ICPMS). Technical Report No. 18, School of Engineering and Science, Jacobs University Bremen.
- Anders E. and Grevesse N. (1989) Abundances of the elements: meteoritic and solar. *Geochim. Cosmochim. Acta* **53**, 197–214.
- Asmerom Y. and Jacobsen S. B. (1993) The Pb isotopic evolution of the Earth: inferences from river water suspended loads. *Earth Planet. Sci. Lett.* **115**, 245–256.
- Bach W. and Irber W. (1998) Rare earth element mobility in the oceanic lower sheeted dyke complex: evidence from geochemical data and leaching experiments. *Chem. Geol.* **151**, 309–326.
- Bau M. (1991) Rare-earth element mobility during hydrothermal and metamorphic fluid–rock interaction and the significance of the oxidation state of europium. *Chem. Geol.* **93**, 219–230.
- Bau M. (1996) Controls on the fractionation of isovalent trace elements in magmatic and aqueous systems: evidence from Y/Ho, Zr/Hf, and lanthanide tetrad effect. *Contrib. Mineral. Petrol.* **123**, 323–333.
- Bau M. (1997) The lanthanide tetrad effect in highly evolved felsic igneous rocks – a reply to the comment by Y Pan. *Contrib. Mineral. Petrol.* **128**, 409–412.
- Bau M. (1999) Scavenging of dissolved yttrium and rare earths by precipitating iron oxyhydroxide: experimental evidence for Ce oxidation, Y–Ho fractionation, and lanthanide tetrad effect. *Geochim. Cosmochim. Acta* **63**, 67–77.
- Bau M. and Alexander B. W. (2009) Distribution of high field strength elements (Y, Zr, REE, Hf, Ta, Th, U) in adjacent magnetite and chert bands and in reference standards FeR-3 and FeR-4 from the Temagami iron-formation, Canada, and the redox level of the Neoproterozoic ocean. *Precambrian Res.* **174**, 337–346.
- Bau M. and Dulski P. (1996a) Anthropogenic origin of positive gadolinium anomalies in river waters. *Earth Planet. Sci. Lett.* **143**, 245–255.
- Bau M. and Dulski P. (1996b) Distribution of yttrium and rare-earth elements in the Penge and Kuruman iron-formations, Transvaal Supergroup, South Africa. *Precambrian Res.* **79**, 37–55.
- Bau M. and Koschinsky A. (2009) Oxidative scavenging of cerium on hydrous Fe oxide: evidence from the distribution of rare earth elements and yttrium between Fe oxides and Mn oxides in hydrogenetic ferromanganese crusts. *Geochem. J.* **43**, 37–47.
- Bau M. and Koschinsky A. (2006) Hafnium and neodymium isotopes in seawater and in ferromanganese crusts: the element perspective. *Earth Planet. Sci. Lett.* **241**, 952–961.
- Bau M., Koschinsky A., Dulski P. and Hein J. R. (1996) Comparison of the partitioning behaviours of yttrium, rare earth elements, and titanium between hydrogenetic marine ferromanganese crusts and seawater. *Geochim. Cosmochim. Acta* **60**, 1709–1725.

- Bau M., Usui A., Pracejus B., Mita N., Kanai Y., Irber W. and Dulski P. (1998) Geochemistry of low-temperature water–rock interaction: evidence from natural waters, andesite, and iron-oxyhydroxide precipitates at Nishiki-numa iron-spring, Hokkaido, Japan. *Chem. Geol.* **151**, 293–307.
- Bau M., Tepe N. and Mohwinkel D. (2013) Siderophore-promoted transfer of rare earth elements and iron from volcanic ash into glacial meltwater, river and ocean water. *Earth Planet. Sci. Lett.* **364**, 30–36.
- Bau M., Schmidt K., Koschinsky A., Hein J., Kuhn T. and Usui A. (2014) Discriminating between different genetic types of marine ferro-manganese crusts and nodules based on rare earth elements and yttrium. *Chem. Geol.* **381**, 1–9.
- Bernhardt P. V. (2007) Coordination chemistry and biology of chelators for the treatment of iron overload disorders. *Dalton Trans.*, 3214–3220.
- Binard N., Maury R. C., Guille G., Talandier J., Gillot P. Y. and Cotten J. (1993) Mehetia Island, South Pacific: geology and petrology of the emerged part of the Society hot spot. *J. Volcanol. Geotherm. Res.* **55**, 239–260.
- Bouby M., Billard I. and MacCordick J. (1998) Complexation of Th (IV) with the siderophore pyoverdine A. *J. Alloys Compd.* **273**, 206–210.
- Boukhalfa H. and Crumbliss A. L. (2002) Chemical aspects of siderophore mediated iron transport. *Biometals* **15**, 325–339.
- Brainard J. R., Strietelmeier B. A., Smith P. H., Langston-Unkefer P. J., Barr M. E. and Ryan R. R. (1992) Actinide binding and solubilization by microbial siderophores. *Radiochim. Acta*, 357–364.
- Brantley S. L., Liermann L., Bau M. and Wu S. (2001) Uptake of trace metals and rare earth elements from hornblende by a soil bacterium. *Geomicrobiol. J.* **18**, 37–61.
- Buss H. L., Lüttge A. and Brantley S. L. (2007) Etch pit formation on iron silicate surfaces during siderophore-promoted dissolution. *Chem. Geol.* **240**, 326–342.
- Choi M.-S., Cho K.-S., Kim D.-S. and Ryu H.-W. (2005) Bioleaching of uranium from low grade black schists by *Acidithiobacillus ferrooxidans*. *World J. Microbiol. Biotechnol.* **21**, 377–380.
- Choppin G. R. (2006) Actinide speciation in aquatic systems. *Mar. Chem.* **99**, 83–92.
- Christenson E. A. and Schijf J. (2011) Stability of YREE complexes with the trihydroxamate siderophore desferrioxamine B at seawater ionic strength. *Geochim. Cosmochim. Acta* **75**, 7047–7062.
- Collerson K. D. and Kamber B. S. (1999) Evolution of the continents and the atmosphere inferred from Th–U–Nb systematics of the depleted mantle. *Science* **283**, 1519–1522.
- Crowe S. A., Døssing L. N., Beukes N. J., Bau M., Kruger S. J., Frei R. and Canfield D. E. (2013) Atmospheric oxygenation three billion years ago. *Nature* **501**, 535–538.
- Dahlheimer S. R., Neal C. R. and Fein J. B. (2007) Potential mobilization of platinum-group elements by siderophores in surface environments. *Environ. Sci. Technol.* **41**, 870–875.
- Davranche M., Pourret O., Gruau G. and Dia A. (2004) Impact of humate complexation on the adsorption of REE onto Fe oxyhydroxide. *J. Colloid Interface Sci.* **277**, 271–279.
- Davranche M., Pourret O., Gruau G., Dia A. and Le Coz-Bouhnik M. (2005) Adsorption of REE(III)-humate complexes onto MnO<sub>2</sub>: experimental evidence for cerium anomaly and lanthanide tetrad effect suppression. *Geochim. Cosmochim. Acta* **69**, 4825–4835.
- Davranche M., Pourret O., Gruau G., Dia a., Jin D. and Gaertner D. (2008) Competitive binding of REE to humic acid and manganese oxide: impact of reaction kinetics on development of cerium anomaly and REE adsorption. *Chem. Geol.* **247**, 154–170.
- Desouky O. A., El-Moughith A. A., Hassanien W. A., Awadalla G. S. and Hussien S. S. (2011) Extraction of some strategic elements from thorium–uranium concentrate using bioproducts of *Aspergillus ficuum* and *Pseudomonas aeruginosa*. *Arab. J. Chem.*
- Dhungana S., White P. S. and Crumbliss A. L. (2001) Crystal structure of ferrioxamine B: a comparative analysis and implications for molecular recognition. *J. Biol. Inorg. Chem.* **6**, 810–818.
- Duckworth O. and Sposito G. (2007) Siderophore-promoted dissolution of synthetic and biogenic layer-type Mn oxides. *Chem. Geol.* **242**, 497–508.
- Duckworth O. W., Bargar J. R. and Sposito G. (2009) Quantitative structure-activity relationships for aqueous metal-siderophore complexes. *Environ. Sci. Technol.* **43**, 343–349.
- Duckworth O. W., Akafia M. M., Andrews M. Y. and Bargar J. (2014) Siderophore-promoted dissolution of chromium from hydroxide minerals. *Environ. Sci. Process Impacts* **6**, 1348–1359.
- Dulski P. (2001) Reference materials for geochemical studies: new analytical data by ICP-MS and critical discussion of reference values. *Geostand. Geoanal. Res.* **25**, 87–125.
- Farkas E., Csóka H., Micera G. and Dessi A. (1997) Copper(II), nickel(II), zinc(II), and molybdenum(VI) complexes of desferrioxamine B in aqueous solution. *J. Inorg. Biochem.* **65**, 281–286.
- Firdaus M. L., Minami T., Norisuye K. and Sohrin Y. (2011) Strong elemental fractionation of Zr–Hf and Nb–Ta across the Pacific Ocean. *Nat. Geosci.* **4**, 227–230.
- Ganesh R., Robinson K. G., Reed G. D. and Sayler G. S. (1997) Reduction of hexavalent uranium from organic complexes by sulfate- and iron-reducing bacteria. *Appl. Environ. Microbiol.* **63**, 4385–4391.
- German C. R. and Elderfield H. (1990) Application of the Ce anomaly as a paleoredox indicator: the ground rules. *Paleoceanography* **5**, 823–833.
- Giese U. and Bau M. (1994) Trace element accessibility in mid-ocean ridge and ocean island basalt: an experimental approach. *Mineral. Mag.* **58A**, 329–330.
- Godfrey L. V., Field M. P. and Sherrell R. M. (2008) Estuarine distributions of Zr, Hf, and Ag in the Hudson River and the implications for their continental and anthropogenic sources to seawater. *Geochemistry Geophys. Geosyst.* **9**.
- Godfrey L. V., White W. M. and Salters V. J. M. (1996) Dissolved zirconium and hafnium distributions across a shelf break in the northeastern Atlantic Ocean. *Geochim. Cosmochim. Acta* **60**, 3995–4006.
- Goldschmidt V. M. (1937) The principles of distribution of chemical elements in minerals and rocks. *J. Chem. Soc.*, 655.
- Grenthe I., Fuger J., Konings R. J. M., Lemire R. J., Muller A. B., Nguyen-Trung Cregu C. and Wanner H. (2004). In *Chemical Thermodynamics of Uranium* (eds. H. Wanner and I. Forest). OECD Publications, Issy-les-Moulineaux.
- Gruau G. G., Dia A., Olivie-Lauquet G., Davranche M. and Pinay G. (2004) Controls on the distribution of rare earth elements in shallow groundwaters. *Water Res.* **38**, 3576–3586.
- Haase K. M., Petersen S., Koschinsky A., Seifert R., Devay C. W., Keir R., Lackschewitz K. S., Melchert B., Perner M., Schmale O., Süling J., Dubilier N., Zielinski F., Fretzdorff S., Garbe-Schönberg D., Westernströer U., German C. R., Shank T. M., Yoerger D., Giere O., Kuever J., Marbler H., Mawick J., Mertens C., Stöber U., Walter M., Ostertag-Henning C., Paulick H., Peters M., Strauss H., Sander S., Stecher J., Warmuth M. and Weber S. (2007) Young volcanism and

- related hydrothermal activity at 5 S on the slow-spreading southern Mid-Atlantic Ridge. *Geochem. Geophys. Geosyst.*, 8.
- Hémond C., Hofmann A. W., Vlastélic I. and Nauret F. (2006) Origin of MORB enrichment and relative trace element compatibilities along the Mid-Atlantic Ridge between 10° and 24°N. *Geochem. Geophys. Geosyst.*, 7, n/a–n/a.
- Hernlem B. J., Vane L. M. and Sayles G. D. (1999) The application of siderophores for metal recovery and waste remediation: examination of correlations for prediction of metal affinities. *Water Res.* **33**, 951–960.
- Jiang S.-Y., Wang R.-C., Xu X.-S. and Zhao K.-D. (2005) Mobility of high field strength elements (HFSE) in magmatic-, metamorphic-, and submarine-hydrothermal systems. *Phys. Chem. Earth Parts A/B/C* **30**, 1020–1029.
- Johannesson K. H. and Lyons W. B. (1994) The rare-earth element geochemistry of Mono-Lake 24 water and the importance of carbonate complexing. *Limnol. Oceanogr.* **39**, 1141–1154.
- Johannesson K. H., Lyons W. B. and Bird D. A. (1994) Rare earth element concentrations and speciation in alkaline lakes from the western U.S.A. *Geophys. Res. Lett.* **21**, 773–776.
- Kalinowski B. E., Oskarsson A., Albinsson Y., Arlinger J., Ödegaard-Jensen A., Andlid T. and Pedersen K. (2004) Microbial leaching of uranium and other trace elements from shale mine tailings at Ranstad. *Geoderma* **122**, 177–194.
- Kiss T. and Farkas E. (1998) Metal-binding ability of desferrioxamine B. *J. Incl. Phenom. Macrocycl. Chem.* **32**, 385–403.
- Kraemer S. M. (2004) Iron oxide dissolution and solubility in the presence of siderophores. *Aquat. Sci. Res. Across Boundaries* **66**, 3–18.
- Kraemer S. M., Duckworth O. W., Harrington J. M. and Schenkeveld W. D. C. (2014) Metallophores and trace metal biogeochemistry. *Aquat. Geochem.*
- Kraemer D., Junge M., Oberthür T. and Bau M. (2015) Improving Recoveries of platinum and palladium from oxidized platinum-group element ores of the Great Dyke, Zimbabwe, using the biogenic siderophore desferrioxamine B. *Hydrometallurgy* **152**, 169–177.
- Liermann L., Kalinowski B., Brantley S. L. and Ferry J. G. (2000) Role of bacterial siderophores in dissolution of hornblende. *Geochim. Cosmochim. Acta* **64**, 587–602.
- Martell A. and Smith R. (2001) *NIST Stability Constants of Metal Complexes Database 46, 6.0*. Gaithersburg, MD.
- Moffett J. W. (1990) Microbially mediated cerium oxidation in sea water. *Nature* **345**, 421–423.
- Möller P. and Bau M. (1993) Rare-earth patterns with positive cerium anomaly in alkaline waters from Lake Van, Turkey. *Earth Planet. Sci. Lett.* **117**, 671–676.
- Mullen L., Gong C. and Czerwinski K. (2007) Complexation of uranium (VI) with the siderophore desferrioxamine B. *J. Radioanal. Nucl. Chem.* **273**, 683–688.
- Müller G., Matzanke B. F. and Raymond K. N. (1984) Iron transport in *Streptomyces pilosus* mediated by ferrichrome siderophores, rhodotorulic acid, and enantio-rhodotorulic acid. *J. Bacteriol.* **160**, 313–318.
- Neaman A., Chorover J. and Brantley S. (2005) Implications of the evolution of organic acid moieties for basalt weathering over geological time. *Am. J. Sci.* **305**, 147–185.
- Newsome L., Morris K. and Lloyd J. R. (2014) The biogeochemistry and bioremediation of uranium and other priority radionuclides. *Chem. Geol.* **363**, 164–184.
- Nick H., Acklin P., Lattmann R., Buehlmayer P., Hauffe S., Schupp J. and Alberti D. (2003) Development of tridentate iron chelators: From desferriothiocin to ICL670. *Curr. Med. Chem.* **10**, 1065–1076.
- Ohnuki T. and Yoshida T. (2012) Interactions of the rare earth elements-desferrioxamine B complexes with *Pseudomonas fluorescens* and  $\gamma$ -Al<sub>2</sub>O<sub>3</sub>. *Chem. Lett.* **41**, 98–100.
- Ohnuki T., Yoshida T., Nankawa T., Ozaki T., Kozai N., Sakamoto F., Suzuki Y. and Francis A. J. (2005) A continuous flow system for in-situ XANES measurements of change in oxidation state of Ce(III) to Ce(IV). *J. Nucl. Radiochem. Sci.* **6**, 65–67.
- Ohta A. and Kawabe I. (2001) REE (III) adsorption onto Mn dioxide ( $\delta$ -MnO<sub>2</sub>) and Fe oxyhydroxide: Ce(III) oxidation by  $\delta$ -MnO<sub>2</sub>. *Geochim. Cosmochim. Acta* **65**, 695–703.
- Ozaki T., Suzuki Y., Nankawa T., Yoshida T., Ohnuki T., Kimura T. and Francis A. J. (2006) Interactions of rare earth elements with bacteria and organic ligands. *J. Alloys Compd.* **408–412**, 1334–1338.
- Pattan J. N., Pearce N. J. G. and Mislankar P. G. (2005) Constraints in using Cerium-anomaly of bulk sediments as an indicator of paleo bottom water redox environment: a case study from the Central Indian Ocean Basin. *Chem. Geol.* **221**, 260–278.
- Pourret O., Davranche M., Gruau G. and Dia A. (2007) Rare earth elements complexation with humic acid. *Chem. Geol.*, 5.
- Qiu G., Li Q., Yu R., Sun Z., Liu Y., Chen M., Yin H., Zhang Y., Liang Y., Xu L., Sun L. and Liu X. (2011) Column bioleaching of uranium embedded in granite porphyry by a mesophilic acidophilic consortium. *Bioresour. Technol.* **102**, 4697–4702.
- Rosenberg D. R. and Maurice P. A. (2003) Siderophore adsorption to and dissolution of kaolinite at pH 3 to 7 and 22 °C. *Geochim. Cosmochim. Acta* **67**, 223–229.
- Rosing M. T. and Frei R. (2004) U-rich Archean sea-floor sediments from Greenland – indications of >3700 Ma oxygenic photosynthesis. *Earth Planet. Sci. Lett.* **217**, 237–244.
- Rudnick R. L., Gao S. (2003) Composition of the Continental Crust. In *Treatise on Geochemistry* Elsevier. pp. 1–64.
- Schmidt K., Bau M., Hein J. R. and Koschinsky A. (2014) Fractionation of the geochemical twins Zr–Hf and Nb–Ta during scavenging from seawater by hydrogenetic ferromanganese crusts. *Geochim. Cosmochim. Acta* **140**, 468–487.
- Schnurr W. (1995) *Spurenelementgeochemie proterozoischer Cherts, Jasper and Jaspilite der Ongeluk Lava und der basalen Hotazel Formation, Kaapvaal Kraton, Südafrika*. RWTH Aachen.
- Shibata S., Tanaka T. and Yamamoto K. (2006) Crystal structure control of the dissolution of rare earth elements in water–mineral interactions. *Geochem. J.* **40**, 437–446.
- Stern J. C., Foustoukos D. I., Sonke J. E. and Salters V. J. M. (2014) Humic acid complexation of Th, Hf and Zr in ligand competition experiments: Metal loading and pH effects. *Chem. Geol.* **363**, 241–249.
- Tanaka K., Tani Y., Takahashi Y., Tanimizu M., Suzuki Y., Kozai N. and Ohnuki T. (2010) A specific Ce oxidation process during sorption of rare earth elements on biogenic Mn oxide produced by *Acremonium* sp. strain KR21-2. *Geochim. Cosmochim. Acta* **74**, 5463–5477.
- Taylor S. R. and McLennan S. M. (1995) The geochemical evolution of the continental crust. *Rev. Geophys.* **33**, 241–265.
- Tepe N. and Bau M. (2014) Importance of nanoparticles and colloids from volcanic ash for riverine transport of trace elements to the ocean: evidence from glacial-fed rivers after the 2010 eruption of Eyjafjallajökull Volcano, Iceland. *Sci. Total Environ.* **488–489**, 243–251.
- Watteau F. and Berthelin J. (1994) Microbial dissolution of iron and aluminium from soil minerals: efficiency and specificity of hydroxamate siderophores compared to aliphatic acids. *Eur. J. Soil Biol.* **30**, 1–9.

- Wilkins M. J., Livens F. R., Vaughan D. J. and Lloyd J. R. (2006) The impact of Fe(III)-reducing bacteria on uranium mobility. *Biogeochemistry* **78**, 125–150.
- Wollf-Boenisch D. and Traina S. (2007) The effect of desferrioxamine B on the desorption of U(VI) from Georgia kaolinite KGa-1b and its ligand-promoted dissolution at pH 6 and 25 °C. *Chem. Geol.* **242**, 278–287.
- Yoshida T., Ozaki T., Ohnuki T. and Francis A. J. (2004) Adsorption of rare earth elements by gamma-Al<sub>2</sub>O<sub>3</sub> and *Pseudomonas fluorescens* cells in the presence of desferrioxamine B: implication of siderophores for the Ce anomaly. *Chem. Geol.* **212**, 239–246.
- Yoshida T., Ozaki T., Ohnuki T. and Francis A. J. (2007) Interactions of trivalent and tetravalent heavy metal-siderophore complexes with *Pseudomonas fluorescens*. *Radiochim. Acta* **92**, 749–753.

*Associate editor:* Jon Chorover